International Journal of Engineering, Mathematical and Physical Sciences
ISSN: 2517-9934
Vol:6, No:11, 2012

Source Optimisation of Laser-Plasma Bremmstrahlung for Applications in Engineering Imaging

R.J. Clarke, D. Neely, S. Blake, D.C. Carroll, J.S. Green, R. Heathcote, and M. Notley

***Abstract*—**High Power Lasers produce an intense burst of Bremmstrahlung radiation which has potential applications in broad-band x-ray radiography. Since the radiation produced is through the interaction of accelerated electrons with the remaining laser target, these bursts are extremely short – in the region of a few ps. As a result, the laser-produced x-rays are capable of imaging complex dynamic objects with zero motion blur.

***Keywords*—**Bremmstrahlung, Imaging, Laser, Plasma, Radiography, x-ray.

I. Introduction

THE production of high-energy Bremmstrahlung radiation from relativistic electron beams in solid targets has been previously reported [1], along with the potential applications for highly penetrating imaging [2]. The radiation produced spans a wide bandwidth from 10's keV up to 40 MeV [1]-[3] and as such can be applicable for a wide range of imaging applications by modifying the target geometry and material. In order to demonstrate the potential for real-world applications, experiments were performed on the Vulcan Petawatt Facility [4] to further investigate the source optimization, stability and capabilities for imaging of both static and dynamic objects.

II. Experimental Configurations

The laser was focused onto solid slabs of tantalum (Ta) ranging in thickness from 20 µm to 6 mm at 45° angle of incidence using p-polarised light. The produced radiation was detected primarily through the use of Thermo Luminescent Device (TLD) stacks similar to those reported in [2] and [3] to determine the dose behind different linear densities of materials. Since the experiment was application driven, the deposited dose measured behind different densities provided the necessary exposure information and as such, a de-convolved photon spectrum was not required. Data was taken at multiple angles, but only those along the laser axis and target normal (rear) are discussed here. Comparisons between data obtained in earlier experimental runs taken in a similar geometry (2011 data) are discussed.

R. J Clarke is with the Central Laser Facility at STFC Rutherford Appleton Laboratory, Oxford, UK, OX11 0QX ; email: rob.clarke@stfc.ac.uk.
All other Authors are also at the Central Laser Facility at STFC Rutherford Appleton Laboratory, Oxford, UK, OX11 0QX.

III. Experimental Analysis

In order to remove contamination on the detectors from electron and proton signals, permanent magnets were used to deflect charged particles out of plane. However, due to restrictions in geometry, a full deflection of the charged particles was not possible and the first TLD layer saw significantly increased signals for targets below thicknesses of 100 µm, suggesting proton contamination. This was confirmed using copper activation measurements through the giant dipole resonance peak of the ^{63}Cu (p,n) ^{63}Zn reaction as described in [5].

The variation of measured dose on TLD 4, behind a linear density of 11.32 g/cm^2 is shown in fig. 1 for 1 mm think Ta targets. The data plots the TLD dose (mGy) per unit Joule of incident laser energy onto the target in order to account for shot-to-shot drive energy variations. For the 1mm thick target data, a set of lower values represent a cluster of shots at lower drive intensities, both from a reduced energy on target and from a stretched laser pulse (5 ps drive pulse instead of ~500fs).

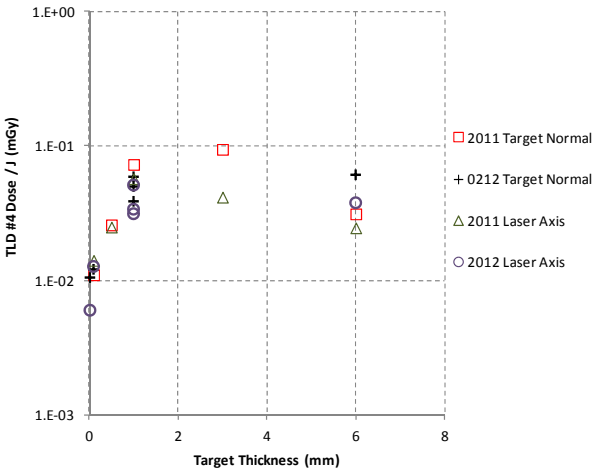

Fig. 1 Measured photon dose (mGy/J) behind 11.32g/cm^2 material as a function of laser-target thickness. Data includes (for 1mm targets) shots at 5ps and reduced energy on target

The shape of the data plotted in fig 1 is representative of all TLD signals, peaking at a target thickness of around 3mm. This shape is consistent with theory, since the laser is

interacting with a thin layer at the front of the target. As the target thickness increases, the relativistically accelerated electrons are converted in greater numbers to high-energy photons, but self-attenuation of the produced radiation from this front layer also increases. As a result, there is a balance between generation and attenuation as the thickness is increased. By normalizing the TLD data to the first TLD channel, the effective radiation "hardness" is apparent. This data (fig. 2) shows how the relative doses behind high linear density increases (indicating a "harder" photon spectrum) with increased target thickness and begins to approach an exponential drop-off as would be expected by a spectrum dominated by 1-10 MeV photons near the peak transmission point of most materials.

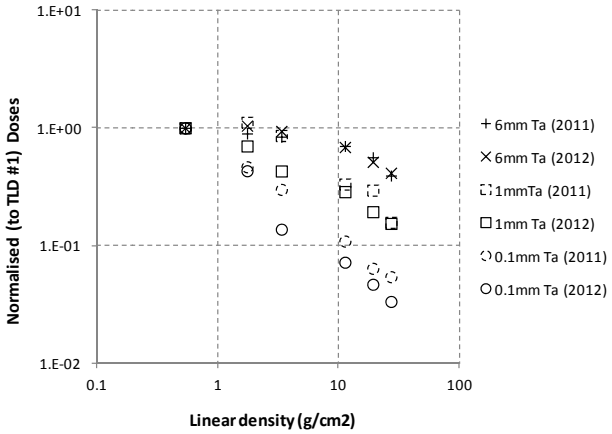

Fig. 2 Normalised photon dose as a function of linear density for different laser-target thickness

As the target thickness is increased, scattering effects within the target lead to a direct increase in the effective source size which, although generating the ability to penetrate higher z materials effectively reduce the available resolution.

IV. Application to Imaging

As part of the experiment, a series of imaging objects were used to assess the viability of the laser-plasma source. Objects were placed around 2 m from the target outside the main vacuum interaction chamber with a 1.5 cm thick vacuum window in front of the objects. The detector was a Fujifilm BAS MS image plate separated from the object by approximately 10 cm and backed by 2 mm of lead to reduce low energy back-scattered radiation. The practical limitations in the geometry at the time limited the ability to optimize this set-up, such as reducing the flange thickness or decreasing the distance from source to object. As a result, a significant part of the low-energy spectrum was attenuated, reducing contrast on thin (or low z) objects.

Two specific objects were radiographed. Firstly, a Cathode Ray Tube (CRT) monitor was imaged at several angles to reconstruct a 3D x-ray image. Since the full 3D image cannot be displayed here, a 2D image is shown in fig 3. This image was taken at full intensity with a 0.1 mm Ta target. The main components and internal wiring is clearly visible throughout, emphasizing the high-resolution (and hence small source) achieved by the laser-produced source.

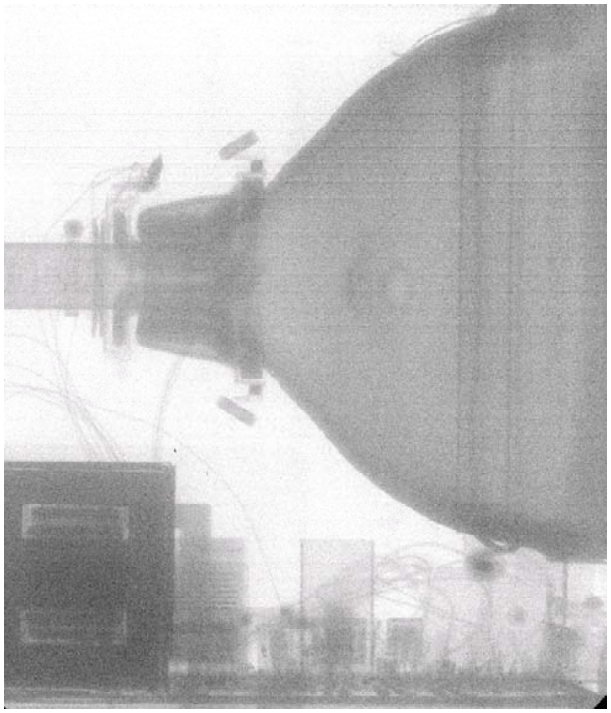

Fig. 3 X-ray radiograph (part of a series for generating a 3D image) of a Cathode Ray Tube (CRT) monitor

In a second series of shots, an Oerlikon Leybold TMP-361 turbo-molecular pump was imaged operating at full speed (45,000 rpm). The image taken with a 0.1 mm Ta target is shown in fig 4 alongside a photo showing the internals of a similar Oerlikon Leybold turbo pump [6]. Even with the thick vacuum window reducing the low energy portion of the photon spectrum the blade definition can still be observed with zero motion blur.

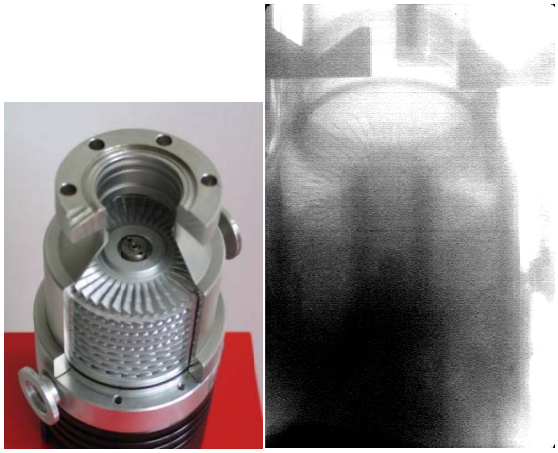

Fig. 4 X-ray radiograph of an Oerlikon Leybold TMP-361 turbo-molecular pump operating at full speed

In order to quantify the effect of target thickness on both the penetration and resolution, the same object was imaged under the same laser conditions but varying the target thickness. A selection of cropped images from the central shaft of the same turbo pump is shown in fig 5. These images highlight two effects of increasing the target thickness. Firstly an increase in transmission through high linear density regions is observed as the x-ray spectrum hardens, with the image contrast for lower density regions being reduced as a result. Secondly a significant reduction in the achievable resolution is seen for thicker targets, possibly due to increased scattering within the target as mentioned in earlier discussions and also detector resolution of the harder spectral components.

V. Conclusion

The application of laser-plasma produced bremmstrahlung radiation for imaging applications has been demonstrated, with target selection highly dependent upon the object to be imaged. Given the ultra-short pulsed nature of the emitted radiation, the laser-plasma source has a unique capability for high speed dynamic imaging.

Acknowledgment

The authors would like to acknowledge the support and expertise of the VULCAN laser facility staff and support teams.

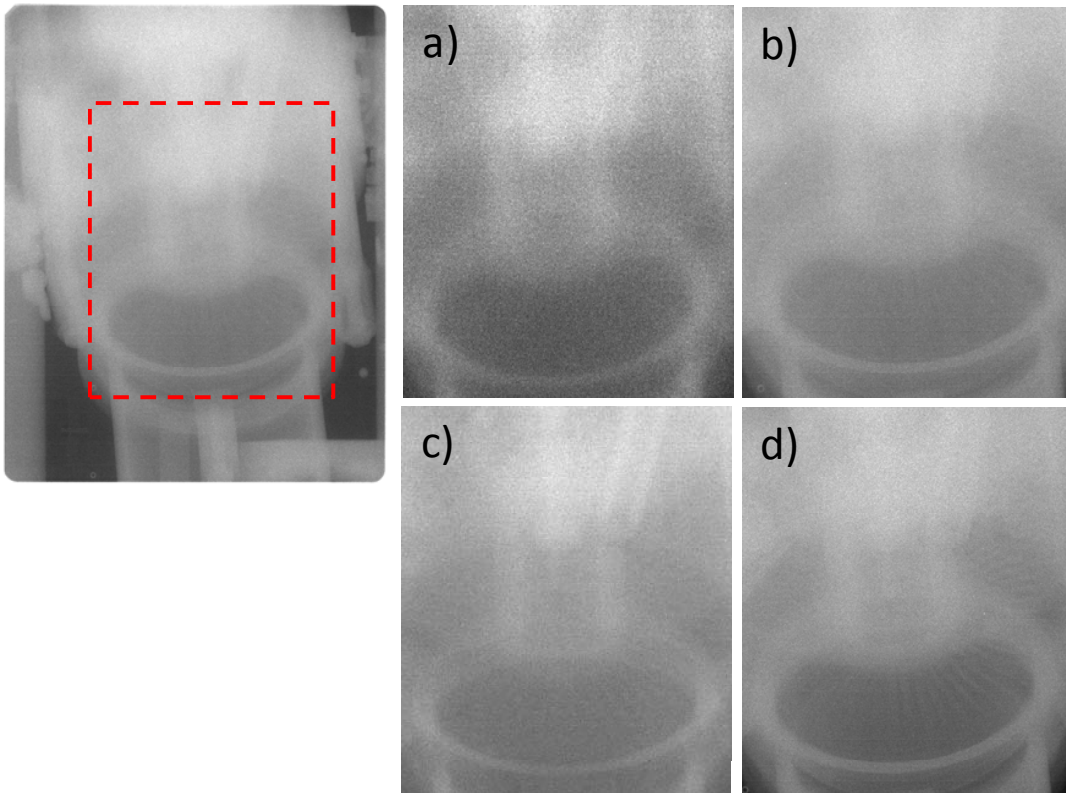

Fig. 5 X-ray radiograph of the pump shaft (static) taken with a) 6mm, b) 3mm, c) 0.5mm and d) 0.1mm Ta targets

References

[1] P. Norreys et al, "Observation of a highly directional gamma ray beam from ultrashort, ultraintense laser pulse interactions with solids." *Physics of Plasmas, 6, 5, (1999);*

[2] R Edwards et al, "Characterization of a gamma-ray source based on a laser-plasma accelerator with applications to radiography." *Appl. Phys. Lett. 80, 2129 (2002);*

[3] R.J. Clarke et al, "Radiological characterisation of photon radiation from ultra-high-intensity laser–plasma and nuclear Interactions" *J. Radiol. Prot.* ***26*** *(2006) 277–286.*

[4] C.N. Danson et al, "Vulcan Petawatt: Design Operation and Interactions at $5x10^{20}$ W/cm^2". *Laser Part. Beams 23, 87-93.*

[5] I. Spencer et al, "Laser generation of proton beams for the production of short-lived positron emitting radioisotopes." *Nucl. Instrum. Methods Phys. Res. B* ***183****, 449 (2001).*

[6] Photo provided by Oerlikon Leybold.